ISSN: 2472-3703 DOI: 10.6911/WSRJ.202105_7(5).0003

Investigation on Thermal Excitation Mechanism of Er^{3+}-doped BaY_2F_8 Single Crystal

Shuai Wang[1, a, *], Yongfeng Ruan[2], Pengfei Wang[1]

[1]School of Science, Shandong Jiaotong University, Jinan, 250357, China

[2]School of Science, Tianjin University, Tianjin, 300072, China

[a]shuaiwangtju@163.com

Abstract

The absorption and emission spectra of thermal coupling levels in Er^{3+}-doped BaY_2F_8 single crystal were measured at room temperature (297 K). The effect of temperature on emission spectra was investigated in the range of 12-297 K. The results show that the intensities of $^4S_{3/2}\rightarrow{}^4I_{15/2}$ (540 nm, 542 nm, 544 nm, 551 nm and 560 nm) Stark level transitions decrease with increasing temperature, while the $^2H_{11/2}\rightarrow{}^4I_{15/2}$ (517 nm, 522 nm, 526 nm and 529 nm) Stark level transitions exhibits the opposite behavior. The thermal excitation mechanism of the Er^{3+} thermal coupling levels will be discussed.

Keywords

Barium yttrium fluoride; Erbium ion; Emission spectrum; Thermal coupling levels; Thermal excitation.

1. INTRODUCTION

Barium yttrium fluoride (BaY_2F_8-BaYF) is a good host material since its very low phonon energy ( ] $\omega \sim$360-380 cm^{-1}) reduces occurrence of non-radiative processes with respect to the radiative ones. In addition, the low refractive index ($n = 1.52$) suggests a low thermal lensing effect, which contributes to the luminescence of the activators. Erbium-doped single crystals play important roles in potential application, such as high-density optical data storage, laser displays, gas detection, etc.

In this paper, we focus on the optical characterization of the thermal coupling levels in Er^{3+}-doped BaY_2F_8 crystal via a combination of absorption and emission. More attentions are paid to revealing the effect of temperature on the optical characterization and analyzing thermal excitation mechanism.

2. EXPERIMENTAL PROCEDURES

The Er^{3+}-doped BaY_2F_8 crystals were grown by temperature gradient method [9-10]. The raw materials were the high-purity synthesized powders (>99.99%) of BaF_2, YF_3 and ErF_3 in stoichiometric amounts. The absorption spectrum was measured by a Shimadu UV-3101 PC spectrometer in the visible ranges (500-600 nm) at room temperature. The tested sample is a slice cutting from Er^{3+}-doped BaY_2F_8 single crystal. The temperature-dependent photoluminescence measurements were carried out from room temperature (RT=297 K) to 12 K on a Spex Fluorolog-3 spectrophotometer in Faculty of Engineering, Kyoto Sangyo University.

ISSN: 2472-3703 DOI: 10.6911/WSRJ.202105_7(5).0003

3. RESULTS AND DISCUSSION

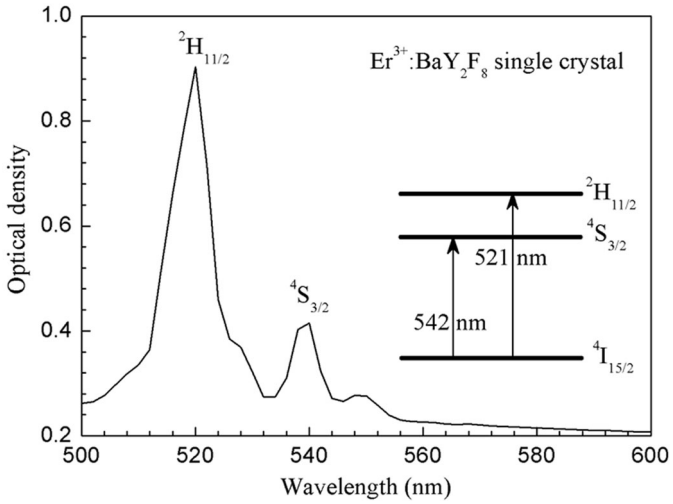

Figure 1. Absorption spectrum of Er^{3+}-doped BaY_2F_8 single crystal at room temperature

Figure 1 shows the absorption spectrum of the thermal coupling levels ($^2H_{11/2}$ and $^4S_{3/2}$) in Er^{3+}-doped BaY_2F_8 single crystal ranging from 500 nm to 600 nm. On the basis of Hund's rules, the ground state of Er^{3+} ions in BaY_2F_8 single crystal is $^4I_{15/2}$. Two absorption bands are observed at 521 nm and 542 nm, which are due to the transitions from the $^4I_{15/2}$ ground state to the $^2H_{11/2}$ and $^4S_{3/2}$ excited states, respectively. The emission spectrum of Er^{3+}-doped BaY_2F_8 single crystal at room temperature with excitation at 375 nm is shown in Figure 2. Several emission peaks are collected and the observed emission peak positions are located at 517 nm, 522 nm, 526 nm, 529 nm, 540 nm, 542 nm, 544 nm, 551 nm and 560 nm. Under the influence of the crystal field, each of the electronic states is split into a certain number of Stark levels. The four emission peaks observed at 517 nm, 522 nm, 526 nm and 529 nm correspond to the $^2H_{11/2} \rightarrow {}^4I_{15/2}$ Stark level transitions. Other five emission peaks observed at 540 nm, 542 nm, 544 nm, 551 nm and 560 nm correspond to the $^4S_{3/2} \rightarrow {}^4I_{15/2}$ Stark level transitions. The Stark-level positions for $^2H_{11/2}$, $^4S_{3/2}$ and $^4I_{15/2}$ of Er^{3+} ions in BaY_2F_8 have been published in Ref. [11]. These data are listed in Table 1.

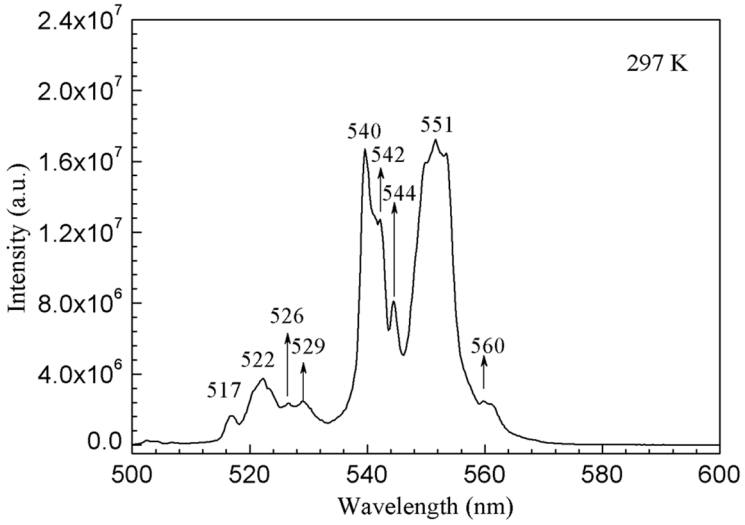

Figure 2. Emission spectrum of Er^{3+}-doped BaY_2F_8 single crystal at room temperature (297 K) obtained upon excitation at 375 nm.

ISSN: 2472-3703 DOI: 10.6911/WSRJ.202105_7(5).0003

Table 1. Stark-level positions for $^2H_{11/2}$, $^4S_{3/2}$ and $^4I_{15/2}$ of Er^{3+} ions in BaY_2F_8

Stark-level number (cm^{-1})	Level number							
	1	2	3	4	5	6	7	8
$^2H_{11/2}$	19,168	19,200	19,232	19,332	19,352	19,371		
$^4S_{3/2}$	18,455	18,552						
$^4I_{15/2}$	0	24	46	102	282	330	372	410

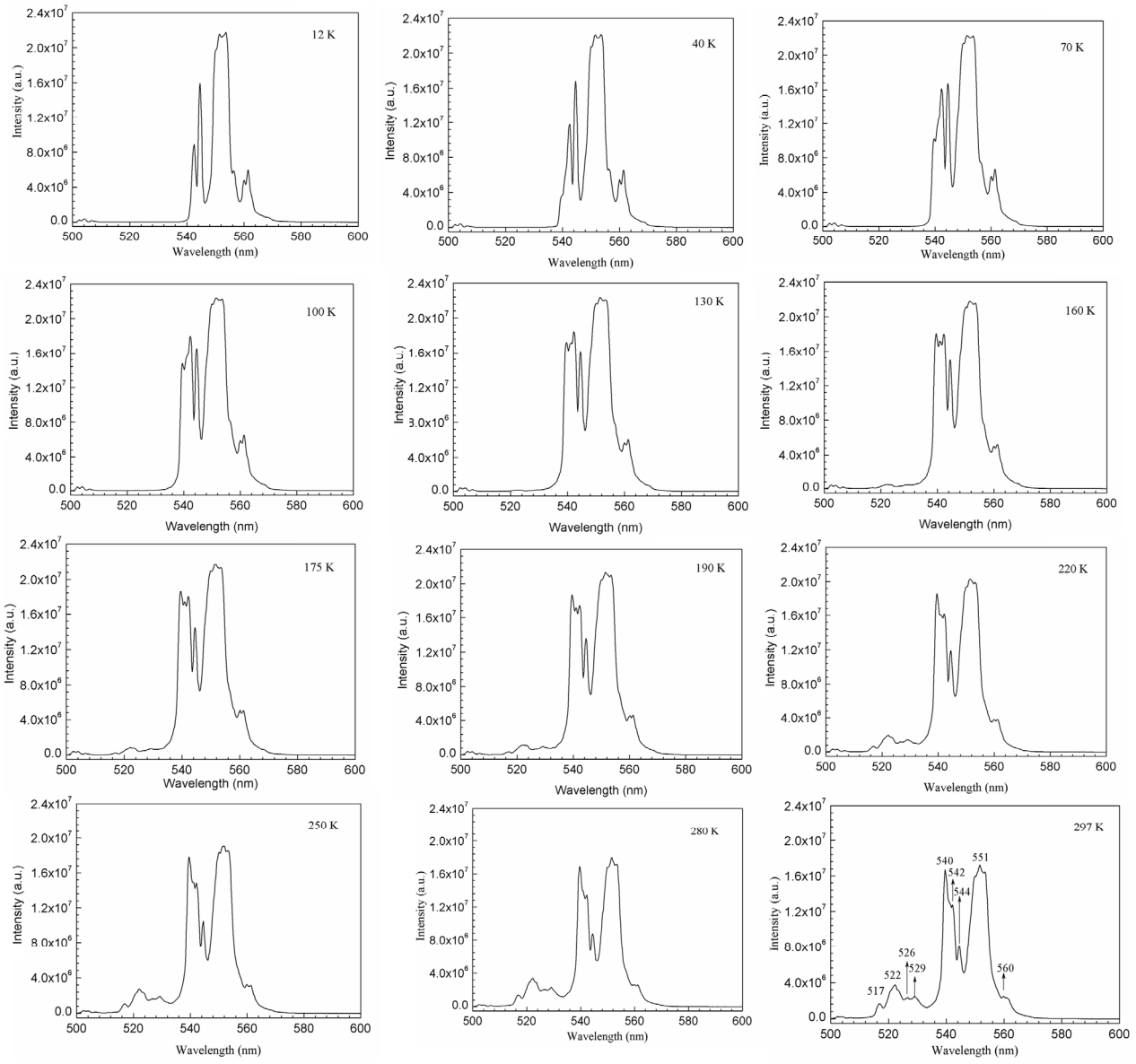

Figure 3. Temperature evolution of the emission spectra from 12 K to 297 K obtained upon excitation at 375 nm.

Figure 3 shows the temperature evolution of the emission spectra from 12 K to 297 K. It is found that the intensities of $^4S_{3/2}\rightarrow{}^4I_{15/2}$ Stark level transitions decrease with increasing temperature, while the $^2H_{11/2}\rightarrow{}^4I_{15/2}$ Stark level transitions exhibits the opposite behavior. It is well known that the density of phonons increases as the temperature rises, which results in stronger electron-phonon interaction. The non-radiative transition probability usually increases with increasing the temperature due to the increasing number of phonons at higher temperature. The stronger electron-phonon interaction makes the low-energy states populated from the high-energy states through the non-radiative transition. The intensity of fluorescence

ISSN: 2472-3703 DOI: 10.6911/WSRJ.202105_7(5).0003

peak usually decreases with increasing temperature. However, the $^2H_{11/2}\rightarrow{}^4I_{15/2}$ Stark level transitions don't obey this rule and they exhibit the opposite behavior. It is believed that there must be another transition mechanism in Er^{3+}-doped BaY_2F_8 single crystal. Based on the absorption spectrum of Er^{3+}-doped BaY_2F_8 single crystal, we consider only the spin-orbit coupling of Er^{3+} ions and do not take account of Stark splitting under the influence of the crystal flied. The energy gap between the $^2H_{11/2}$ and $^4S_{3/2}$ states is about 1042 cm^{-1}. Such a narrow energy gap means that the $^2H_{11/2}$ state can be populated from the $^4S_{3/2}$ state by the thermal excitation. The possible thermally coupled levels mechanisms of the BaY_2F_8 crystal doped with Er^{3+} ions under 375 nm excitation is depicted in Figure 4.

When the Er^{3+}-doped BaY_2F_8 crystals are excited, the Er^{3+} ion at the $^4I_{15/2}$ ground state absorbs a 375 nm photon and populates the higher metastable states. Subsequently, the Er^{3+} ion at the higher metastable states populate the $^2H_{11/2}$ state and the $^4S_{3/2}$ state through the non-radiative transition or radiative transition. Due to the narrow energy gap between $^2H_{11/2}$ and $^4S_{3/2}$ states (~1042 cm^{-1}), the $^2H_{11/2}$ state can be populated from the $^4S_{3/2}$ state by the thermal excitation under the help of the phonons. With increasing the temperature, the $^4S_{3/2}$ state loses its population, whereas the population of the $^2H_{11/2}$ state increases under the influence of the thermal excitation. The overall effect is that the population of the $^2H_{11/2}$ state is larger than that of the $^4S_{3/2}$ state and the relaxation rate of the $^2H_{11/2}$ state is smaller than that of the $^4S_{3/2}$ state. Therefore the intensity of $^2H_{11/2}\rightarrow{}^4I_{15/2}$ (517 nm, 522 nm, 526 nm and 529 nm) transition increases and that of $^4S_{3/2}\rightarrow{}^4I_{15/2}$ (540 nm, 542 nm, 544 nm, 551 nm and 560 nm) transition decreases with increasing the temperature.

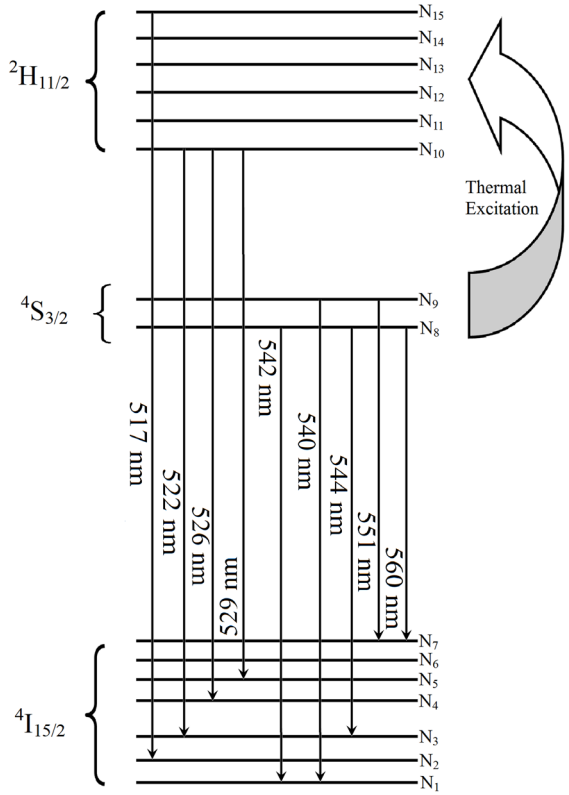

Figure 4. Thermal excitation mechanisms of the Er^{3+}-doped BaY_2F_8 crystal

4. CONCLUSIONS

In summary, the absorption and emission spectra of the Er^{3+}-doped BaY_2F_8 single crystal were measured at room temperature. The temperature dependence of optical characterization has been demonstrated in the range of 12-297 K. The results show that the intensities of

ISSN: 2472-3703 DOI: 10.6911/WSRJ.202105_7(5).0003

$^4S_{3/2}\rightarrow{}^4I_{15/2}$ (540 nm, 542 nm, 544 nm, 551 nm and 560 nm) Stark level transitions decrease with increasing temperature, while the $^2H_{11/2}\rightarrow{}^4I_{15/2}$ (517 nm, 522 nm, 526 nm and 529 nm) Stark level transitions exhibits the opposite behavior. The thermal excitation mechanism of the Er^{3+} thermal coupling levels also has been discussed.

ACKNOWLEDGMENTS

We thank Wenrun Li and Liangang Li at Tianjin University for providing the help.

We are also very grateful to Zhouli Wu at NAURA Technology Group Co., Ltd.

REFERENCES

[1] X.C. Yu, F. Song, C.G. Zou, et al. Temperature dependence of luminescence behavior in Er^{3+}/Yb^{3+} co-doped transparent phosphate glass ceramics, Optical Materials, 2009, 31: 1645-1649.

[2] O. Svelto. Principles of Lasers, third ed., Plenum, New York, 1989. pp. 70-71.

[3] H. Berthou, C.K. Jorgenson. Optical-fiber temperature sensor based on upconversion-excited fluorescence, Optics Letters, 1990, 15(19): 1100-1102.

[4] P.V. dos Santos, M.T. Araujo, A.S. Gouveia-Neto, et al. Optical temperature sensing using upconversion flourescence emission in Er^{3+}/Yb^{3+}-codoped chalcogenide glass, Appl. Phys. Lett., 1998, 73: 578-580.

[5] S.A. Wade, S.F. Collins, and G.W. Baxter. The fluorescence intensity ratio technique for optical fiber temperature sensing, J. Appl. Phys., 2003, 94: 4743-4756.

[6] S.S. Andrea, D. Camargo et al, Infrared to visible frequency upconversion temperature sensor based on Er^{3+}-doped PLZT transparent ceramics, Solid State Communications, 2006, 137: 1-5.

[7] B. Dong, X.S. Xu, X.J. Wang, T. Yang and Y.Y. He. Infrared-to-visible upconversion emissions and thermometric applications of Er^{3+}-doped Al_2O_3, Applied Physics B, 2007, 89: 281-284.

[8] B. Dong, D.P. Liu, X.J. Wang, T. Yang, S.M. Miao and C.R. Li, Optical thermometry through infrared excited green upconversion emissions in Er^{3+}/Yb^{3+} codoped Al_2O_3, Applied Physics Letters, 2007, 90(18):1-3.

[9] S. Wang, Y.F. Ruan, T.J. Tsuboi, et al.Investigation on growth and macro-defects of Er^{3+}-doped BaY_2F_8 laser crystal, Journal of Crystal Growth, 2013, 376: 47-53.

[10] S. Wang, Y.F. Ruan, T.J. Tsuboi, et al. Studies on the growth and optical characterizaition of Tm^{3+}-doped BaY_2F_8 single crystal, Crytstal Research and Technology, 2012, 47: 9928-9938.

[11] A. Baraldi, R. Capelletti, M. Mazzera, A. Ponzoni, G. Amoretti, N. Magnani, A. Toncelli, M. Tonelli, Phys. Rev. B 72 (2005) 075132.